

Effect of La doping on structural, magnetic and microstructural properties of $\text{Ba}_{1-x}\text{La}_x\text{Fe}_{12}\text{O}_{19}$ ceramics prepared by citrate combustion process

S. Ounnunkad · P. Winotai · S. Phanichphant

© Springer Science + Business Media, LLC 2006

Abstract La-substituted M-type barium ferrites, $\text{Ba}_{1-x}\text{La}_x\text{Fe}_{12}\text{O}_{19}$, with $x = 0.00\text{--}0.30$ were successfully prepared via a citrate combustion process. Properties of the ceramics were characterized by powder X-ray diffraction, vibrating sample magnetometry and scanning electron microscopy. XRD patterns revealed only magnetoplumbite structure without minor phases. With increasing the La substituted content, the saturation magnetization (M_S) was increased and reached to a maximum at $x = 0.15$ and then decreased but coercivity (H_C) was increased. SEM micrographs of the dense ceramics showed the hexagonal platelet shape at low La content and the irregular shape at high La content.

Keywords Barium ferrites · Hysteresis loops · Magnetization · Coercivity

1 Introduction

Ferrimagnetic barium hexaferrite with magnetoplumbite (M) structure is revealed and the general formula $\text{BaFe}_{12}\text{O}_{19}$ has been considered as a permanent magnet which applied for electronic material industry [1, 2]. It demonstrates good properties such as an application in high frequency and high tem-

perature with low price, great heat resistance, and high corrosion resistance in comparison with those of ferromagnetic alloys [3]. The hexaferrite can be also used in a variety of magnetic and electronic devices such as high density perpendicular recording media, in communications, electronic power generation, automotive electronics, microwave devices, and ferrite core [1, 4–6].

The magnetic properties can be enhanced by using optimization in the synthetic conditions [7–11], synthetic routes and special impurity element additions. Various chemical processes have usually been adopted to prepare the excellent pure and doped barium hexaferrites such as hydrothermal [7], sol-gel [8, 12], co-precipitation [10, 13], microwave-induced combustion [14] and citrate-nitrate gel auto-combustion process [15]. These chemical syntheses show high purity of the barium ferrite phase, uniform grain, chemical homogeneity and good magnetic properties. Moreover, many studies have also been concerned with cationic substitutions. Usually, many cations and various cationic combinations are used in doping into barium hexaferrites, belonging to their applications such as Co-Ti-Mn and Mn-Ti substitutions for the microwave absorbers [5], Zn-Ti, Co-Sn, Co-Ti and Cr or Y doping for high density magnetic recording applications [11, 13, 16, 17] and Co, Cr, Mn, Ni and Pr-Ni additions for magneto-optical applications [18, 19].

Recently, it is interesting that a new family of the ferrites doped with rare earth ions showed the required properties. The microwave behavior of spinel ferrites was improved by substitution of Ru and Gd for Fe^{3+} ion sites [20]. Insertion of Gd or Pr into Fe lattices inhibited grain growth, reduced grain size and controlled the coercive force for wide practical applications [21]. Corral Huacuz et al. [22] and Du et al. [23] found that La-Zn substitution greatly modified the magnetic properties and microstructure of barium ferrites. These substituted

S. Ounnunkad (✉) · S. Phanichphant
Nanoscience Research Laboratory, Department of Chemistry,
Faculty of Science, Chiang Mai University, Chiang Mai 50200,
Thailand
e-mail: sounnunkad@yahoo.com; suriyacmu@yahoo.com

P. Winotai
Department of Chemistry, Faculty of Science, Mahidol
University, Rama VI Rd., Bangkok 10400, Thailand

hexaferrites yielded more homogeneous microstructure and fine crystallite sizes compared with pure specimen. Moreover, Wang et al. [24] and Grössinger et al. [25] showed the substitution of Sm ions giving fine M ferrite powders and resulting increase in coercivity. Furthermore, the light rare earth ions (Re) were used in substitution for Sr (Ba) and Fe, respectively, taking into account the ionic radius of the elements and enhancing magnetic parameters [26]. Ba^{2+} or Sr^{2+} site replaced by a Re^{3+} ion can be associated with a valence of one Fe^{3+} to Fe^{2+} ion per formula unit [26].

In this paper, the effect of La ions on structural, microstructural and magnetic properties of La-substituted barium ferrite ceramics, $\text{Ba}_{1-x}\text{La}_x\text{Fe}_{12}\text{O}_{19}$ ($0.00 \leq x \leq 0.30$) is discussed. The substitution of La^{3+} ions on the Ba^{2+} sites can strongly influence magnetic properties, i.e., saturation magnetization and coercive field strength.

2 Experimental details

The $\text{Ba}_{1-x}\text{La}_x\text{Fe}_{12}\text{O}_{19}$ ferrites, with $x = 0.00$ – 0.30 were prepared by a combustion process using nitric acid as an oxidant and citric acid as a fuel. The stoichiometric mixture solution of metal ions was prepared by dissolving BaCO_3 , $\text{La}(\text{NO}_3)_3 \cdot 6\text{H}_2\text{O}$, $\text{Fe}(\text{NO}_3)_3 \cdot 9\text{H}_2\text{O}$ and citric acid in acidic deionized water. The homogenous solution was slowly evaporated at 160°C and then the viscous brown gel was obtained. The gel precursor was ignited and combusted by increasing the temperature up to 250°C . The resulting black ashes were calcined at 1100°C for 1 h in flowing oxygen gas and then the calcined powders were ground, sieved through 200 meshes, and die-pressed at 2,000 psi in a 1.2 mm diameter die. The green bodies were also sintered at 1300°C for 12 h in an oxygen atmosphere.

Magnetoplumbite phase was examined from powder X-ray diffraction (XRD) using a Bruker Axs Diffractometer with $\text{CuK}\alpha$ radiation. Both lattice parameters were identified by using FULLPROF-SUITE 2000 package program

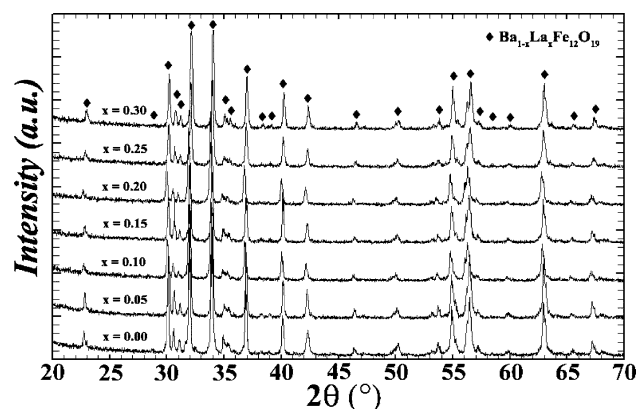


Fig. 1 XRD patterns of $\text{Ba}_{1-x}\text{La}_x\text{Fe}_{12}\text{O}_{19}$ ceramics

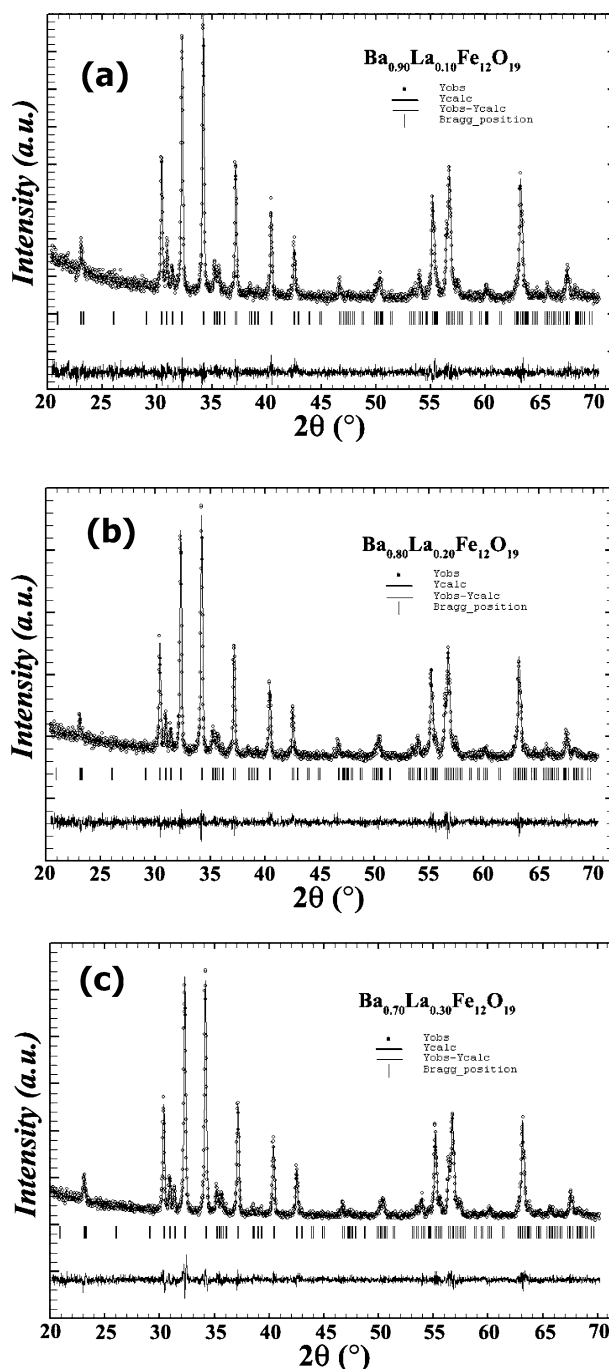


Fig. 2 Simulated XRD patterns for (a) $\text{Ba}_{0.90}\text{La}_{0.10}\text{Fe}_{12}\text{O}_{19}$, (b) $\text{Ba}_{0.80}\text{La}_{0.20}\text{Fe}_{12}\text{O}_{19}$ and (c) $\text{Ba}_{0.70}\text{La}_{0.30}\text{Fe}_{12}\text{O}_{19}$

with profile matching. Magnetic hystereses were recorded by using LAKESHORE vibrating sample magnetometer (VSM) and saturation magnetizations were calculated by law of approach to saturation with magnetic field range from 8.0 to 10.0 kOe [16, 27]. Morphology and grain size were studied by a HITACHI S-2500 scanning electron microscope (SEM).

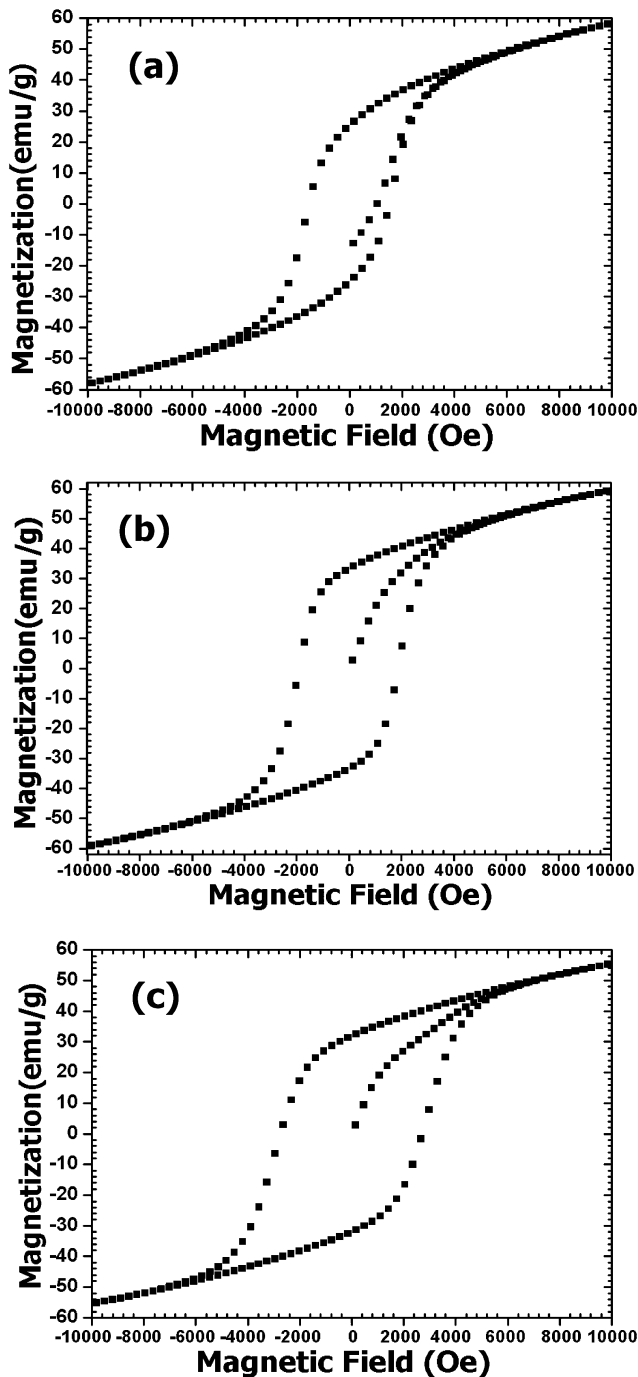


Fig. 3 Hystereses for (a) $\text{Ba}_{0.95}\text{La}_{0.05}\text{Fe}_{12}\text{O}_{19}$, (b) $\text{Ba}_{0.80}\text{La}_{0.20}\text{Fe}_{12}\text{O}_{19}$ and (c) $\text{Ba}_{0.70}\text{La}_{0.30}\text{Fe}_{12}\text{O}_{19}$

3 Results and discussion

Figure 1 shows that all room temperature XRD patterns of sintered hexaferrites with various La contents are in monophasic magnetoplumbite phase which conformed with the reference to $\text{BaFe}_{12}\text{O}_{19}$ without any intermediate phases such as $\alpha\text{-BaFe}_2\text{O}_4$ (barium spinel ferrite), BaFeO_3 (barium orthoferrite), $\alpha\text{-Fe}_2\text{O}_3$ (hematite), LaFeO_3 (lanthanum

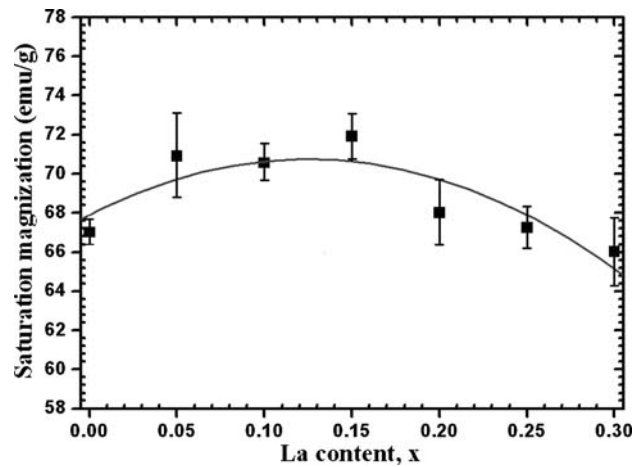


Fig. 4 Saturation magnetizations of $\text{Ba}_{1-x}\text{La}_x\text{Fe}_{12}\text{O}_{19}$ ceramics

orthoferrite), La_2O_3 and $\gamma\text{-Fe}_2\text{O}_3$ (maghemite). Typical XRD patterns of the prepared single phase ceramics were successfully identified, as shown in Fig. 2. The XRD patterns correspond to Bragg positions of the magnetoplumbite structure having hexagonal symmetry with space group $P6_3/mmc$. Both lattice parameters (a and c), unit cell volumes and Bragg R -factors of the ceramics are listed in Table 1. The cell volume of pure sample is smaller than those of doped samples. This may suggest that it has a higher crystallinity and La ions may be difficult to form as the solid state solution.

Figure 3 illustrates the magnetic properties can be associated with the typical field-dependent magnetizations, i.e., hysteresis loops. They are of the hard magnetic characteristic with high coercive field strength. In the applied magnetic field range (from -10 kOe to 10 kOe), the magnetizations of the ferrites were not saturated. Thus, the saturation magnetizations (M_S) were deduced from the equation of law of approach to saturation when using magnetic field range of $\sim 8.0\text{--}10.0$ kOe [16, 27]. It was found that the ferrite pellets showed an abnormal magnetic behavior with respect to La content. At the beginning the M_S increased, up to a maximum ($x = 0.15$) and then decreased dramatically, as exhibits in Fig. 4. This could be considerably noted that the increase in the M_S due to spin canting caused by La^{3+} ions, which

Table 1 Refined lattice parameters and Bragg R -factor for $\text{Ba}_{1-x}\text{La}_x\text{Fe}_{12}\text{O}_{19}$ ceramics

x	a (Å)	c (Å)	c/a	Cell volume (Å ³)	Bragg R -factor
0.00	5.8740	23.1265	3.9371	691.058	5.67
0.05	5.8815	23.1621	3.9381	693.885	6.94
0.10	5.8836	23.1718	3.9384	694.659	4.21
0.15	5.8829	23.1593	3.9367	694.122	6.61
0.20	5.8832	23.1354	3.9324	693.483	4.24
0.25	5.8888	23.1436	3.9301	695.048	4.64
0.30	5.8878	23.1253	3.9277	694.252	4.11

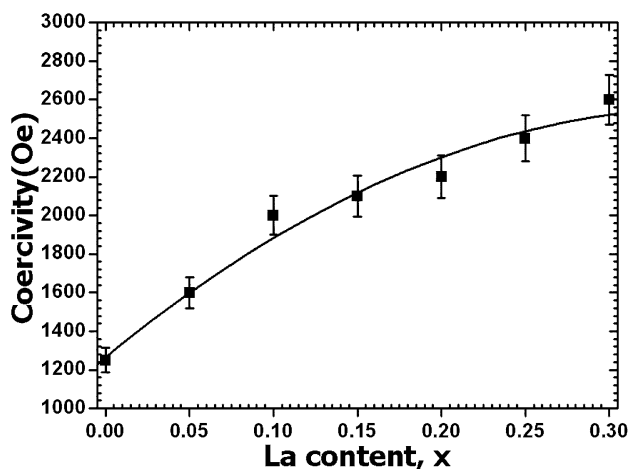


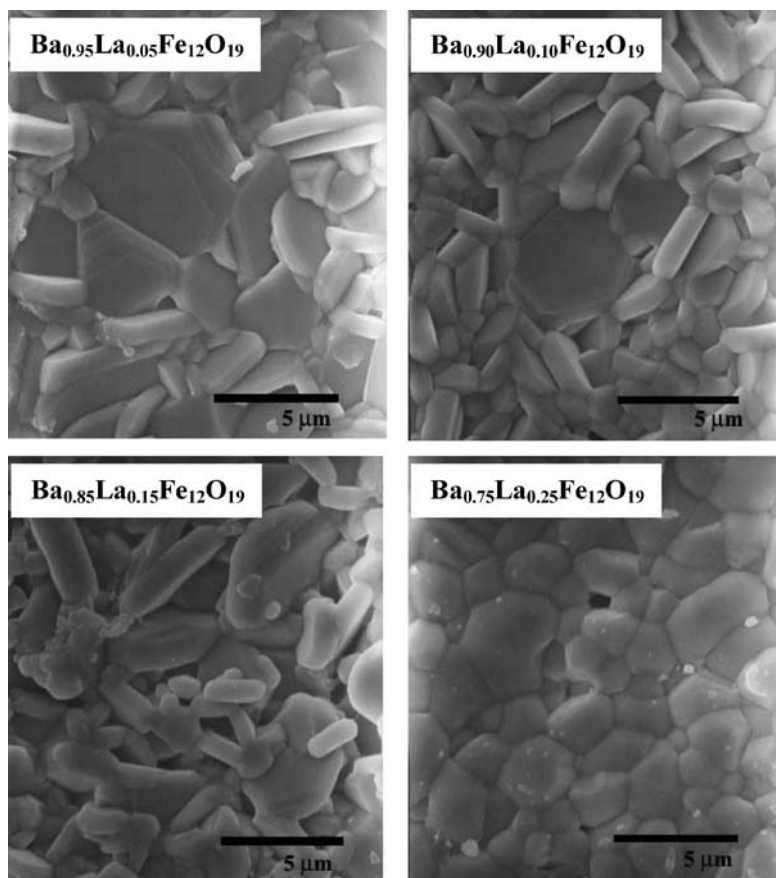
Fig. 5 Coercive field strengths of $\text{Ba}_{1-x}\text{La}_x\text{Fe}_{12}\text{O}_{19}$ ceramics

deviated from the collinear to a non-collinear arrangement had been occurred [28]. The enlargement in hyperfine field strength at Fe crystallographic sites might contribute to the increase in M_S [26, 28]. In addition, the decrease in the M_S was due to a Fe^{3+} ($3d^5$ high spin) ion forming into Fe^{2+} state ($3d^6$ low spin) per substitution of one La^{3+} ion, giving a weakened $\text{Fe}^{3+}\text{-O-Fe}^{3+}$ superexchange interaction and dilution

of internal magnetic field strength. Therefore, the optimum La substitution fraction of synthesized hexaferrites ceramics was at a composition of $x = 0.15$. In comparison with La-doped strontium ferrites [26, 28], the optimum La contents are identical.

The coercive field strength (H_C) (in the order of $\sim 1\text{--}2.5$ kOe) remarkably increases with increasing La concentration, as illustrated in Fig. 5. Normally, the enhancement of coercivity could be found in rare earth substitutions into the hexaferrites only, suggesting an increase in the magnetocrystalline anisotropy constant and reduction of grain size. This study suggested that La ions enter into the solid solution to enhance magnetocrystalline anisotropy constant and inhibit grain growth mechanism. Surprisingly, SEM micrographs showed the transformation of grain morphology with no change in crystal structure. At low doping content, grain shapes were of hexagonal platelets with hexagonal diameter (on a - b plane) and thickness (along c -axis), as in the pure sample. On the other hand, at high La content the irregular shape was occurred. The SEM micrographs of the dense sintered bodies showed hexagonal and irregular shapes in the order of $\sim 2\text{--}5$ μm in diameters, as shown in Fig. 6. The average grain sizes of the dense ceramics were smaller and the morphology was changed as Ba sites were substituted by La ions.

Fig. 6 SEM micrographs of $\text{Ba}_{1-x}\text{La}_x\text{Fe}_{12}\text{O}_{19}$ ceramics



4 Conclusion

The hexaferrite ceramics from citrate combustion process showed the optimum La content to improve the M_S at composition of $x = 0.15$. In this doping range ($0.00 \leq x \leq 0.30$), the La^{3+} ions diffused into a crystal structure and formed as pure M ferrite phase. M_S increased at first and then decreased but H_C systematically increased with respect to La addition. As of the magnetic property result, the disruption of La^{3+} ions on $\text{Fe}^{3+}\text{-O-Fe}^{3+}$ superexchange interaction contributed to the behavior of magnetization. With increasing La^{3+} ions, the grain morphology could be changed from hexagonal platelet-like shape to irregular or spherical shape without changing in the crystalline structure.

Acknowledgments The authors would like to thank The Development and Promotion for Science and Technology Talents Project of Thailand (DPST), the Postgraduate Education and Research Program in Chemistry (PERCH), Graduate School and Department of Chemistry, Faculty of Science, Chiang Mai University for financial supports and Assoc. Prof. Dr. Sujittra Youngmee, Department of Chemistry, Faculty of Science, Khon Kaen University for providing the VSM facility.

References

1. R.A. McCurrie, *Ferromagnetic Materials: Structure and Properties* (Academic Press, London, 1994), p. 155 & 234.
2. S.R. Janasi, D. Rodrigues, F.J.G. Landgraf, and M. Emura, *IEEE Trans Magn.*, **36**(5), 3327 (2000).
3. M. Sugimoto, *J. Am. Ceram. Soc.*, **82**(2), 269 (1999).
4. H. Kojima, in *Fundamental Properties of Hexagonal Ferrites: Ferromagnetic Materials*, edited by E.P. Wohlfarth (New York, North-Holland, 1982), p. 305.
5. M.R. Meshram, N.K. Agrawal, B. Sinha, and P.S. Misra, *J. Magn. Mater.*, **271**, 207 (2004).
6. G.K. Thompson and B.J. Evans, *J. Appl. Phys.*, **73**(10), 6295 (1993).
7. X. Liu, J. Wang, L.-M. Gan, and S.-C. Ng, *J. Magn. Magn. Mater.*, **195**, 452 (1999).
8. G. Mendoza-Suárez, M.C. Cisneros-Morales, M.M. Cisneros-Guerrero, K.K. Jahal, H. Mancha-Molinar, O.E. Ayala-Valenzuela, and J.I. Escalante-García, *Mater. Chem. Phys.*, **77**, 796 (2002).
9. H.-F. Yu and K.-C. Huang, *J. Magn. Magn. Mater.*, **260**, 455 (2003).
10. S.R. Janasi, M. Emura, F.J.G. Landgraf, and D. Rodrigues, *J. Magn. Mater.*, **238**, 168 (2002).
11. F. Wei, M. Lu, and Z. Yang, *J. Magn. Magn. Mater.*, **191**, 249 (1999).
12. R.C. Pullar and A.K. Bhattachaya, *Mater. Lett.*, **57**, 537 (2002).
13. P.C. Kuo, Y.D. Yao, and W.I. Tzang, *J. Appl. Phys.*, **73**(10), 6292 (1993).
14. Y.-P. Fu, C.-H. Lin, and K.-Y. Pan, *Jpn. J. Appl. Phys.*, **42**(5A), 2681 (2003).
15. J. Huang, H. Zhuang, and W. Li, *J. Magn. Magn. Mater.*, **256**, 390 (2003).
16. Z. Yang, H.-X. Zeng, D.-H. Han, J.-Z. Liu, and S.-L. Geng, *J. Magn. Mater.*, **115**, 77 (1992).
17. Y.J. Chen and M.H. Kryder, *J. Appl. Phys.*, **79**(8), 4878 (1996).
18. R. Carey, P.A. Gago-Sandoval, D.M. Newman, and B.W.J. Thomas, *J. Appl. Phys.*, **75**(10), 6789 (1994).
19. M. Gomi, J. Cho, and M. Abe, *J. Appl. Phys.*, **82**(10), 5126 (1997).
20. S.E. Jacobo, W.G. Fano, and A.C. Razzitte, *Physica B*, **320**, 261 (2002).
21. R. N. Panda, J. C. Shih, and T.S. Chin, *J. Magn. Magn. Mater.*, **257**, 79 (2003).
22. J.C. Corral-Huacuz and G. Mendoza-Suárez, *J. Magn. Magn. Mater.*, **242–245**, 430 (2002).
23. Y.-W. Du, H.-X. Lu, Y.-C. Zhang, and T.-X. Wang, *J. Magn. Magn. Mater.*, **31–34**, 793 (1983).
24. J.F. Wang, C.B. Ponton, and I.R. Harris, *J. Magn. Magn. Mater.*, **242–245**, 1464 (2002).
25. R. Grössinger, C.T. Blanco, M. Küpferling, M. Müller, and G. Wiesinger, *Physica B*, **327**, 202 (2003).
26. X. Liu, W. Zhong, S. Yang, Z. Yu, B. Gu, and Y. Du, *Phys. Stat. Sol. (a)*, **193**(2), 314 (2002).
27. B.D. Cullity, *Introduction to Magnetic Materials* (Addison-Wesley, Massachusetts, 1972), p. 347.
28. X. Liu, W. Zhong, S. Yang, Z. Yu, B. Gu, and Y. Du, *J. Magn. Magn. Mater.*, **238**, 207 (2002).